Three interacting atoms in a one-dimensional trap: A benchmark system for computational approaches

Pino D'Amico and Massimo Rontani

E-mail: pino.damico@nano.cnr.it, massimo.rontani@nano.cnr.it
CNR-NANO Research Center S3, Via Campi 213/a, 41125 Modena, Italy

Abstract. We provide an accurate calculation of the energy spectrum of three atoms interacting through a contact force in a one-dimensional harmonic trap, considering both spinful fermions and spinless bosons. We use fermionic energies as a benchmark for exact-diagonalization technique (also known as full configuration interaction), which is found to slowly converge in the case of strong interatomic attraction.

PACS numbers: 67.85.-d, 31.15.ac, 03.75.Ss, 67.85.Lm

Submitted to: *J. Phys. B: At. Mol. Phys.*

1. Introduction

Experimental advances allow us to confine a chosen number of few quantum degenerate atoms in a trap with unit precision. Whereas this capability was first demonstrated for bosons in optical lattices [1,2], the Heidelberg group applied a spilling technique to subtract ^{6}Li fermionic atoms one by one from a single trap, down to the zero limit [3–6]. Due to the strong anisotropy of the magneto-optical trap employed, the few-atom system was effectively one-dimensional. The tunability of both confinement potential and interaction—the latter achieved by sweeping a magnetic offset field through a Feshbach resonance [7]—opens new avenues to understand interacting particles in one dimension [8–14].

So far the experiments [3–6] have revealed that phenomena previously investigated in the presence of many atoms may be studied in the limit of few particles as well, as the Fermi-Bose duality [4, 15, 16] (also known as 'fermionization' [17, 18]), the formation of the Fermi polaron [6, 19–21], the emergenge of pairing [5, 9, 22–26]. This has fueled theoretical proposals that are specific to few-atom traps, focusing on themes as diverse as Stoner ferromagnetism [27–32], exchange mechanisms [33,34], Wigner localization [35, 36], quasiparticle- [37] and pair-tunneling [38], the Fulde-Ferrell-Larkin-Ovchinnikov state [39], pairing [40], mesoscopic phase separations for bosons [41]. On one hand, the study of few interacting atoms, which are the bulding blocks of many-body states, gives an insight into the essential physical features of more complex quantum systems. On the other hand, the few-body problem may be analyzed using fully understood theoretical models [42, 43] that provide a benchmark for approximate theories fit to larger numbers of particles.

In this paper we report accurate calculations of the energy spectra of few atoms interacting through contact forces in a one-dimensional harmonic trap. Since an analytic solution (recalled in section 2) is available for two particles [44], we consider three atoms, which are either spinful fermions or spinless bosons. Our approach is based on a well controlled variational method (VM)—inspired by previous work in two [45] and three [27] dimensions—that is physically transparent, since the three-atom basis set is made of the exact two-body wave functions [44] plus one-body spectator orbitals. We then use the VM spectrum as a benchmark for state-of-the-art exact diagonalization [also known as full configuration interaction (CI)], which is the technique of choice for accurate calculations of few-body systems. The CI basis set is simpler than the VM one, as it is made of the Slater determinants obtained by filling with three fermions a truncated set of trap orbitals, consistently with Pauli exclusion principle. The comparison between VM and CI data points to the slow convergence of CI in the regime of strong attractive interactions, highlighting the challenging nature of theories of pairing in few Fermi-atom systems.

The CI technique uniquely accesses energies and wave functions of both ground and excited states, at the price of being limited to few atoms due to the exponential increase of the Hilbert space size with the number of particles [46, 47]. Together with quantum Monte Carlo [9, 48–51], CI provides the ground-state energy with—in principle–arbitrary accuracy, hence it has been widely applied to one-dimensional systems of finite size [28, 30, 31, 33, 36, 39, 46, 52–65]. However, for strong attractive interactions, the two-body wave function tends to collapse in space [44], hence the convergence of the calculation should be carefully assessed. An accurate calculation of the spectrum of three interacting fermions, based on Green function's formalism, was provided by Blume and coworkers [32,66]. These authors investigated the dimensional

crossover from a three-dimensional to a quasi one-dimensional trap but reported partial data for stricly one-dimensional fermions and no data for bosons. Other approaches for three particles in a trap in one dimension include group-theoretical [67] and geometrical analyses [68], multiconfigurational time-dependent Hartree method [63, 69–71], ansatz correlated wave functions [63, 71], effective-interaction approaches [29, 70], density functional theory [72], as well as exact results in the limit of infinite repulsion [34, 73, 74].

This article is organized as follows: in section 2 we work out the analytical solution for two atoms based on the Bethe-Peierls boundary condition, as a preliminary to the three-body problem that is introduced in section 3. In sections 4 and 5 we derive the energy spectra for fermions and bosons, respectively, focusing on the limit of strong repulsion in section 6. In section 7 we compare three-fermion energies with those obtained from CI calculations employing different single-particle basis sets. After the conclusion (section 8), Appendix A presents an alternative derivation of the two-body solution and Appendix B explains the calculation of the matrix elements that occur in the equations for the three-body problem.

2. Two-body problem

As a preliminary step, it is convenient to recall the exact solution of the two-body problem with contact interaction in a one-dimensional trap. Whereas in Appendix A we work out this solution following the original calculation by Busch and coworkers [44], in this section we present an alternative approach based on the application of the Bethe-Peierls boundary condition. We will extend this method to three atoms in sections 4 and 5.

In a trap with tight transverse confinement, the low-energy dynamics is effectively one-dimensional. The hamiltonian H_{2p} for two particles has the following form:

$$H_{2p} = \frac{\bar{p}_1^2 + \bar{p}_2^2}{2m} + \frac{1}{2} m\omega^2 (\bar{x}_1^2 + \bar{x}_2^2) + \bar{g}\delta(\bar{x}_1 - \bar{x}_2), \tag{1}$$

where m is the atom mass, ω is the frequency of the harmonic oscillator, $\bar{g}$ is the interaction strength of the contact interaction, $\bar{p} = i\hbar\partial/\partial\bar{x}$. Throughout the paper we place bars over certain quantities having physical dimensions to discriminate them from their dimensionless counterparts. Physically, the contact interaction is a pseudopotential which mimics Van der Waals inter-atomic interaction at low energies [75]. The handle to tune $\bar{g}$ is the relation [76]

$$\bar{g} = \frac{2\hbar^2 a_{3\mathrm{D}}}{\mu \ell_\perp^2} \frac{1}{1 - C a_{3\mathrm{D}}/\ell_\perp}, \tag{2}$$

where $\mu = m/2$ is the reduced mass, $a_{3\mathrm{D}}$ is the three-dimensional scattering length, $\ell_\perp$ is the harmonic-oscillator length in the transverse direction, $C = 1.4603\ldots = \zeta(1/2)$ with ζ being Riemann's zeta function. A change in the magnetic offset field through a Feshbach resonance modifies $a_{3\mathrm{D}}$, and hence $\bar{g}$. It is clear from (2) that the vanishing of the denominator—a resonance due to the tranverse confinement—allows to reach the "unitarity" limit, $|\bar{g}| \to \infty$, going from $\bar{g} = -\infty$ to $\bar{g} = \infty$ or vice versa by a small field variation.

Because the interaction in Hamiltonian (1) is short-ranged, it affects only two fermions having opposite spins, hence the solution is the same as the one for spinless bosons. It is useful to decouple center-of-mass and relative motions by introducing

the coordinates $\bar{X} = (\bar{x}_1 + \bar{x}_2)/2$ and $\bar{x} = \bar{x}_1 - \bar{x}_2$, hence the total Hamiltonian is the sum of two terms,

$$H_{2p} = H_{\bar{X}} + H_{\bar{x}}, \tag{3}$$

with

$$H_{\bar{x}} = \frac{\bar{p}^2}{2\mu} + \frac{1}{2}\mu\omega^2\bar{x}^2 + \bar{g}\delta(\bar{x}), \tag{4}$$

and

$$H_{\bar{X}} = \frac{\bar{P}^2}{2M} + \frac{1}{2}M\omega^2\bar{X}^2, \tag{5}$$

where the center-of-mass term (5) is a non-interacting harmonic oscillator with doubled mass $M = 2m$ and energy $E_{\bar{X}} = \hbar\omega(n + 1/2)$, with $n = 0, 1, 2, \ldots$ Furthermore, by using $\hbar\omega$ as energy unit and $\ell = (\hbar/\mu\omega)^{1/2}$ as length unit, we introduce in the relative-motion frame the dimensionless variables $\bar{E}_{\bar{x}} = (\hbar\omega)E_x$, $\bar{g} = (\hbar\omega\ell)g$, $\bar{x} = \ell x$, $\bar{p} = (\hbar/\ell)\, p$, with $p = i\partial/\partial x$. Therefore, the total wave function is the product of the non-interacting center-of-mass oscillator times the interacting wave function $\psi(x)$ that obeys the eigenvalue equation

$$\left[\frac{p^2}{2} + \frac{x^2}{2} + g\delta(x)\right]\psi(x) = E_x\psi(x). \tag{6}$$

There are two ways to solve the eigenvalue problem (6). One way is to expand the wave function $\psi(x)$ over the eigenstates of the non-interacting problem, i.e. the states of the harmonic oscillator

$$R_n(x) = \frac{1}{\sqrt{2^n n!}}\left(\frac{1}{\pi}\right)^{\frac{1}{4}} \mathrm{e}^{-\frac{x^2}{2}} H_n(x)\,, \tag{7}$$

with $H_n(x)$ being the Hermite polynomial of order n. This approach follows the original derivation by Busch and coworkers [44] and is detailed in Appendix A. In this section we take a different path and match the generic solutions of (6) in the two half-spaces $x < 0$ and $x > 0$ by means of the (Bethe-Peierls) contact condition [77],

$$\frac{\partial\psi(0^+)}{\partial x} - \frac{\partial\psi(0^-)}{\partial x} = 2g\psi(0). \tag{8}$$

We write the generic solution of Eq. (6) with $x \neq 0$ as

$$\psi(x) = e^{-\frac{x^2}{2}} f(x), \tag{9}$$

with $f(x)$ to be determined. Setting the relative-motion energy to $E_x = (2\nu + 1/2)$ the eigenvalue problem (6) is reduced to

$$\frac{\partial^2 f(x)}{\partial x^2} - 2x\frac{\partial f(x)}{\partial x} + 4\nu f(x) = 0. \tag{10}$$

With the transformation $z = x^2$ we obtain

$$z\frac{\partial^2 f(z)}{\partial z^2} + \left(\frac{1}{2} - z\right)\frac{\partial f(z)}{\partial z} + \nu f(z) = 0. \tag{11}$$

Expression (11) is Kummer's equation with parameters $a = -\nu$ and $b = 1/2$, the solutions being Kummer's functions $M(-\nu, 1/2, x^2)$ and $U(-\nu, 1/2, x^2)$ [78]. The contact condition (8) imposes that the solution has a singular derivative at the origin. Since $M(-\nu, 1/2, x^2)$ is proportional to the Hermite polynomial and hence

has continuous derivatives at $x = 0$ whereas those of $U(-\nu, 1/2, x^2)$ are singular, the generic solution in the whole space is

$$\psi(x) = \mathrm{e}^{-\frac{x^2}{2}} U\left(-\nu, \frac{1}{2}, x^2\right), \tag{12}$$

that is the same as Eq. (A.14) except for a normalization constant.

To find the eigenvalues, we recall a few properties of Kummer's function U in the limit $x \to 0$ [78]:

$$U\left(-\nu, \frac{1}{2}, x^2\right) = \frac{\Gamma(1/2)}{\Gamma(-\nu + 1/2)} + O(|x|), \tag{13a}$$

$$U\left(-\nu + 1, \frac{3}{2}, x^2\right) = \frac{1}{|x|} \frac{\Gamma(1/2)}{\Gamma(-\nu + 1)} + O(1), \tag{13b}$$

$$\frac{\partial U(a, b, x)}{\partial x} = -a\, U(a + 1, b + 1, x)\,. \tag{13c}$$

Using (13c) we obtain the wave function derivative:

$$\frac{\partial}{\partial x}\psi(x) = 2x\nu U\left(-\nu + 1, \frac{3}{2}, x^2\right) \mathrm{e}^{-\frac{x^2}{2}} + \\ - x\psi(x). \tag{14}$$

Applying (13b) for vanishing x we get

$$\frac{\partial}{\partial x}\psi(x)_{x\to 0^{\pm}} = -2\frac{\sqrt{\pi}}{\Gamma(-\nu)}\mathrm{sign}(x), \tag{15}$$

and using the condition (8) we obtain the eigenvalue equation,

$$\frac{\Gamma(-\nu)}{\Gamma\left(-\nu + 1/2\right)} = -\frac{2}{g}, \tag{16}$$

linking the interaction strenght g to the energy E_x since $E_x = 2\nu + 1/2$.

The resulting energy spectrum, which is plotted in figure 1, exhibits peculiar features. First, the lowest energy branch drops to $-\infty$ for strong attractive interactions, the wave function collapsing in space. Second, the unitarity limit $|g| \to \infty$ shows the fermionization of the interacting energy spectrum, which tends to the noninteracting values that are peculiar of the spin-polarized system, $E_x = 3/2, 7/2, 11/2, \ldots$, whereas the missing values $E_x = 5/2, 9/2, 13/2, \ldots$ are obtained trhough successive center-of-mass excitations. Indeed, the wave function in the relative frame is even, displaying a bosoniclike behavior, hence for strong repulsion it is expected to exhibit the same observable properties as fully polarized fermions that are noninteracting. The same behavior is expected in the presence of strong attraction but only for 'super-Tonks-Girardeau' excited states [73, 74, 79, 80], as the lowest collapsing state has no fermionic counterpart. Experimentally, the ground-state energy branch on the attractive side ($g < 0$) was probed for fermions in Ref. [5] whereas that on the positive side close to $g \to \infty$ was measured in Ref. [4]. The latter experiment also accessed the super-Tonks-Girardeau first excited energy branch close to $g \to -\infty$.

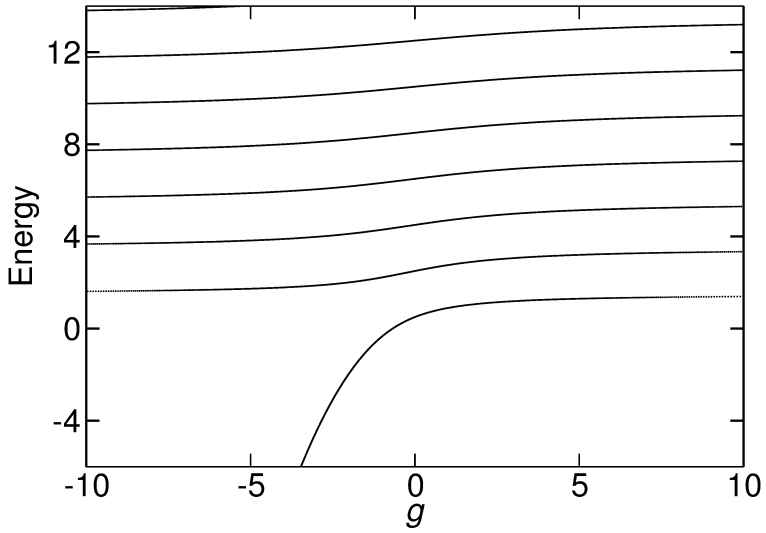

Figure 1. Relative-motion energy of two atoms, E_x, vs interaction strength, g. The energy is in units of $\hbar\omega$ and g in units of $\hbar\omega\ell$.

3. Three-body problem

In this section we introduce the three-atom problem and set the basis of our variational method, which is inspired by the work of Drummond and coworkers in two- [45] and three-dimensional [27] traps. In sections 4 and 5 we specialize the method to fermions and bosons, respectively.

The Hamiltonian is:

$$H_{3p} = \frac{\bar{p}_1^2 + \bar{p}_2^2 + \bar{p}_3^2}{2m} + \frac{1}{2}m\omega^2\left(\bar{x}_1^2 + \bar{x}_2^2 + \bar{x}_3^2\right) + \bar{g}\left[\delta(\bar{x}_1 - \bar{x}_2) + \delta(\bar{x}_1 - \bar{x}_3) + \delta(\bar{x}_2 - \bar{x}_3)\right]. \quad (17)$$

After introducing the Jacobi coordinates,

$$\begin{aligned} \bar{X} &= \frac{\bar{x}_1 + \bar{x}_2 + \bar{x}_3}{3}, \\ \bar{x} &= \bar{x}_1 - \bar{x}_2, \\ \bar{y} &= \frac{2}{\sqrt{3}}\left(\bar{x}_3 - \frac{\bar{x}_1 + \bar{x}_2}{2}\right), \end{aligned} \quad (18)$$

the operator (17) is decoupled into three terms:

$$H_{3p} = H_{\bar{X}} + H_{\bar{x}} + H_{\bar{x}\bar{y}}, \quad (19)$$

with

$$\begin{aligned} H_{\bar{X}} &= \frac{\bar{P}^2}{2M} + \frac{1}{2}M\omega^2\bar{X}^2, \\ H_{\bar{x}} &= \frac{\bar{p}_x^2}{2\mu} + \frac{1}{2}\mu\omega^2\bar{x}^2 + \bar{g}\,\delta(\bar{x}), \\ H_{\bar{x}\bar{y}} &= \frac{\bar{p}_y^2}{2\mu} + \frac{1}{2}\mu\omega^2\bar{y}^2 + \bar{g}\,\delta\Big((\bar{x} - \sqrt{3}\bar{y})/2\Big) + \bar{g}\,\delta\Big((\bar{x} + \sqrt{3}\bar{y})/2\Big), \end{aligned} \quad (20)$$

and $M = 3m$, $\mu = m/2$. As for two atoms, the center-of-mass motion is a harmonic oscillation decoupled from the relative motion. Using again as unit length ℓ and unit energy $\hbar\omega$, the eigenvalue problem for the relative motion, in terms of dimensionless variables, is

$$(H_x + H_{xy})\,\psi_{\rm rel}(x,y) = E\,\psi_{\rm rel}(x,y). \tag{21}$$

Explicitly, Eq. (21) reads as

$$\left[\frac{p_x^2}{2} + \frac{x^2}{2} + g\delta(x) + \frac{p_y^2}{2} + \frac{y^2}{2} + g\,G(x,y)\right]\psi_{\rm rel} = E\,\psi_{\rm rel}, \tag{22}$$

with the shorthand

$$G(x,y) = \delta\Big((x-\sqrt{3}y)/2\Big) + \delta\Big((x+\sqrt{3}y)/2\Big).$$

The system is schematically represented in figure 2.

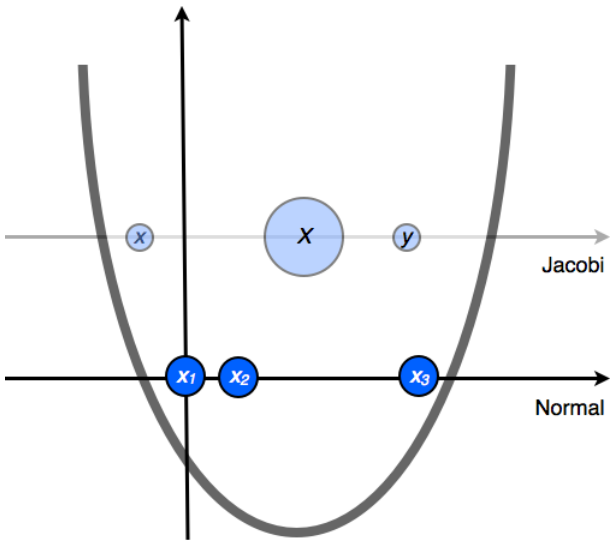

Figure 2. Pictorial representation of three atoms in a harmonic trap. In the usual laboratory frame the three atoms (depicted as circles) have like masses. In the Jacobi reference frame the coordinates represent collective motions with equivalent masses, which are depicted as circles whose radius sizes are proportional to the masses.

In the absence of the interaction term $G(x,y)$, the solution of (22) is the product of the two-atom relative-motion wave function $\psi(x)$ times the harmonic-oscillator solution $R_n(y)$. The term $G(x,y)$ couples x and y degrees of freedom, hence the generic solution of (22) is

$$\Omega(x,y) = \sum_{n=0}^{\infty} a_n \psi_n(x) R_n(y), \tag{23}$$

which relies on the completeness of the basis $\{\psi_n(x)R_n(y)\}_n$. The next two sections are devoted to determine the unknown coefficients a_n in (23) after imposing the Bethe-Peierls contact condition—the analog of (8)—and the proper symmetry under particle exchange.

In the following we normalize $\psi_n(x)$ as:

$$\psi_n(x) = \Gamma(-\nu_n)\, \mathrm{e}^{-\frac{x^2}{2}} U\left(-\nu_n, \frac{1}{2}, x^2\right), \tag{24}$$

where, for fixed n and E, the index ν_n entering the functional form of $\psi_n(x)$ is dictated by the energy conservation,

$$E = \left(2\nu_n + \frac{1}{2}\right) + \left(n + \frac{1}{2}\right) = 2\nu_n + n + 1. \tag{25}$$

4. Three fermions

The wave function $\psi_{\mathrm{rel}}(x, y) \equiv \psi_{3F}(x, y)$ for three fermionic atoms must fullfill the Pauli principle. Identifing the particles with the indices $\{123\}$, we specify the spin configuration choosing e.g. $\{\uparrow\downarrow\uparrow\}$ (the fully polarized system is not interacting), hence atoms 1 and 3 are indistinguishable. Exchanging particles 1 and 3 causes the following coordinate transformation:

$$\begin{aligned} x &\to \frac{x}{2} + \frac{\sqrt{3}}{2} y \equiv \xi, \\ y &\to \frac{\sqrt{3}}{2} x - \frac{y}{2} \equiv \eta. \end{aligned} \tag{26}$$

Therefore, the ansatz

$$\psi_{3F}(x, y) = \Omega(x, y) - \Omega(\xi, \eta) \tag{27}$$

has the correct symmetry, since it changes sign under the $1 \leftrightarrow 3$ swap. This is immediate by writing $\psi_{3F}(x, y)$ as

$$\psi_{3F}(x, y) = (1 - \boldsymbol{P}_{13})\Omega(x, y), \tag{28}$$

where $\boldsymbol{P}_{13}$ is the exchange operator.

The wave function $\psi_{3F}(x, y)$ must also have a definite parity under the inversion operator $\boldsymbol{R}$ that changes the sign of all coordinates, $\boldsymbol{R}\{x_1, x_2, x_3\} = \{-x_1, -x_2, -x_3\}$. This condition is easily realized noticing that the transformation (26) is linear and homogeneous, hence $\boldsymbol{R}\{x, y\} = \{-x, -y\}$, and that $\psi_n(x)$ is even in x. Therefore, the inversion leads to

$$\begin{aligned} \boldsymbol{R}\,\psi_{3F}(x, y) &= \Omega(-x, -y) - \Omega(-\xi, -\eta) \\ &= \Omega(x, -y) - \Omega(\xi, -\eta) \\ &= \sum_{n=0}^{\infty} (-1)^n a_n \left[\psi_n(x) R_n(y) - \psi_n(\xi) R_n(\eta)\right], \end{aligned} \tag{29}$$

showing that the parity of $\psi_{3F}(x, y)$ depens on that of the harmonic-oscillator states R_n by choosing only terms with even (odd) indices in the sum (29).

To find the expansion coefficients a_n we impose on $\psi_{3F}(x, y)$ the Bethe-Peierls contact condition for two fermions of opposite spin approaching each other. For fermions 1 and 2 one has

$$\left[\frac{\partial \psi_{3F}(x, y)}{\partial x}\right]_{x \to 0^+} - \left[\frac{\partial \psi_{3F}(x, y)}{\partial x}\right]_{x \to 0^-} = 2g\, \psi_{3F}(0, y). \tag{30}$$

For fermions 2 and 3 one has

$$\begin{aligned} x_2 &\to x_3, \\ x &\to x_1 - x_3, \\ y &\to \frac{2}{\sqrt{3}}\left[x_3 - \frac{x_1+x_3}{2}\right] = \frac{x_3-x_1}{\sqrt{3}} = -\frac{x}{\sqrt{3}}, \end{aligned}$$

hence

$$\begin{aligned} \xi &\to \frac{x}{2} - \frac{\sqrt{3}}{2}\frac{x}{\sqrt{3}} = 0 \\ \eta &\to \frac{\sqrt{3}}{2}x + \frac{x}{2\sqrt{3}} = \frac{2}{\sqrt{3}}x. \end{aligned}$$

Therefore, the second contact condition is

$$\left[\frac{\partial\psi_{3F}}{\partial\xi}\right]_{\xi\to 0^+} - \left[\frac{\partial\psi_{3F}}{\partial\xi}\right]_{\xi\to 0^-} = 2g\left[\psi_{3F}\right]_{\xi=0}. \tag{31}$$

It turns out that (31) is automatically satisfied once (30) is enforced due to the exchange symmetry of ψ_{3F}.

To apply the condition (30) we note that the derivative of Eq. (27) is

$$\frac{\partial}{\partial x}\psi_{3F}(x,y) = \frac{\partial}{\partial x}\Omega(x,y) - \frac{1}{2}\left[\frac{\partial}{\partial\xi}\Omega(\xi,\eta) + \sqrt{3}\frac{\partial}{\partial\eta}\Omega(\xi,\eta)\right], \tag{32}$$

where the last two terms on the righ-hand side of the above equation have continuos derivative at $x = 0$ and hence do not contribute to the contact constraint. We only need the following derivative:

$$\frac{\partial}{\partial x}\Omega(x,y) = \frac{\partial}{\partial x}\sum_n a_n\psi_n(x)R_n(y) = \sum_n a_n\left[\frac{\partial}{\partial x}\psi_n(x)\right]R_n(y). \tag{33}$$

Using Eqs. (13c) and (13b) for vanishing x as in section 2 we obtain

$$\frac{\partial}{\partial x}\psi_n(x)_{x\to 0^\pm} = -2\sqrt{\pi}\,\mathrm{sign}(x). \tag{34}$$

Noting that

$$\psi_{3F}(x=0) = \Omega(0,y) - \Omega\left(\frac{\sqrt{3}}{2}y, -\frac{y}{2}\right), \tag{35}$$

expanding it close to $x = 0$ using (13a), and combining it with (34), the Bethe-Peierls condition (30) becomes

$$\begin{aligned} &2g\sum_n a_n\left[\sqrt{\pi}\frac{\Gamma(-\nu_n)}{\Gamma(-\nu_n+1/2)}R_n(y) - \psi_n\left(\frac{\sqrt{3}}{2}y\right)R_n\Big(-\frac{y}{2}\Big)\right] \\ &= -4\sqrt{\pi}\sum_n a_n R_n(y), \end{aligned} \tag{36}$$

with the indices appearing in (36) being either even or odd depending on the parity of ψ_{3F}. Exploiting the orthonormality of the orbitals $R_n(y)$, the eigenvalue problem (36) may be written as a set of linear equations,

$$\sum_n F_{mn}\,a_n = -\frac{2\sqrt{\pi}}{g}a_m, \tag{37}$$

with the matrix F_{mn} being defined as

$$F_{mn} = \sqrt{\pi}\frac{\Gamma(-\nu_n)}{\Gamma(-\nu_n+1/2)}\delta_{nm} - A_{mn}, \tag{38}$$

with

$$A_{mn} = \int_{-\infty}^{\infty} \mathrm{d}y\, R_m(y)\, \psi_n\left(\frac{\sqrt{3}}{2}y\right) R_n\Big(-\frac{y}{2}\Big)\,. \tag{39}$$

Note that, when putting $A_{mn} = 0$, one recovers the two-body eigenvalue equation (16), as A_{mn} is the matrix element of the interaction between the pair of atoms in the state ν_n and the "spectator" atom in level m.

The eigenvalue E is hidden in the linear system (37) through the index $\nu_n = (E-n-1)/2$ entering F_{mn}. Practically, to solve the problem we adopt the following procedure: We first choose a cutoff for the size of the linear system (37), with $n = 0, 2, 4, \ldots, n_{\max}$ for even parity and $n = 1, 3, 5, \ldots, n_{\max}+1$ for odd parity, respectively. We then fix E and hence ν_n, evaluate the matrix A_{mn} as explained in Appendix B, solve numerically the eigenevalue problem (37) to obtain the allowed values of g, and iterate the procedure for a different value of E. We eventually invert the relation $g(E)$ and find the energy branches as a function of the interaction strength g, after removing trivial results corresponding to non-interacting states. The latter correspond to fully spin-polarized states after a rotation in the spin space.

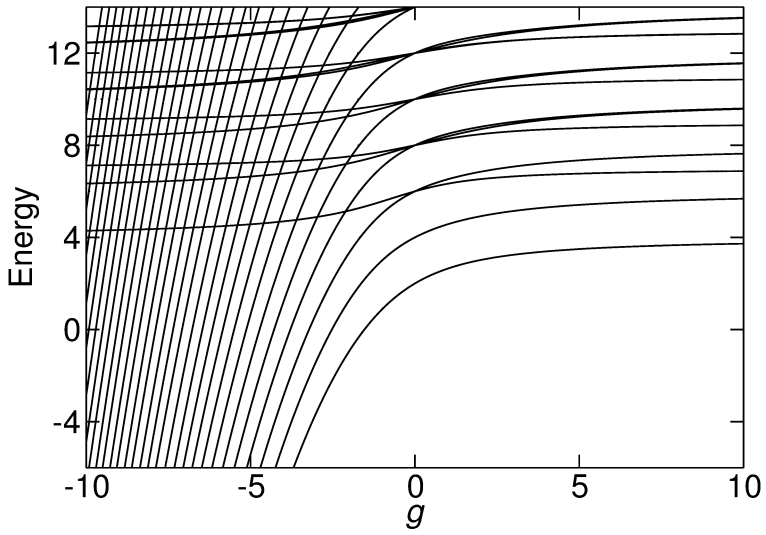

Figure 3. Energy of three fermions vs interaction strength g in the relative frame for states having odd parity. The energy is in units of $\hbar\omega$ and g in units of $\hbar\omega\ell$.

Figures 3 and 4 show the energy spectra for odd and even parity, respectively, obtained with $n_{\max} = 60$, which allows the convergence of the sixth digit of the ground-state energy. With respect to the two-atom spectrum of figure 1, the plots exhibit new qualitative features. First, the orbital states may be either odd (figure 3) or even (figure 4), the former including the absolute ground state. Second, there are two distinct sets of branches in each plot, whose behavior qualitatively differs as $g \to -\infty$: (i) many branches drop towards $-\infty$ (ii) others tend asymptotically to integer values.

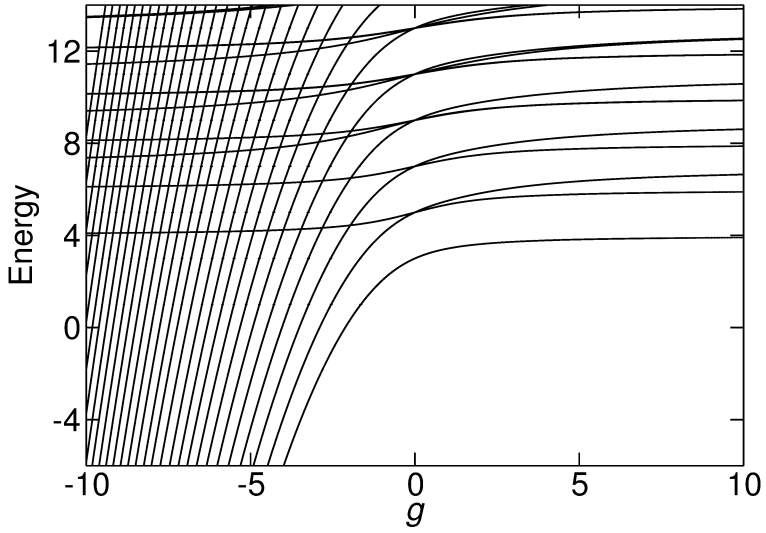

Figure 4. Energy of three fermions vs interaction strength g in the relative frame for states having even parity. The energy is in units of $\hbar\omega$ and g in units of $\hbar\omega\ell$.

The former may be understood as ground-state replicas that are made of two atoms in a strongly-bound state and the third spectator atom occupying consecutive quasiparticle levels of increasing energy. The latter tend to the 'fermionized' values of the fully spin-polarized state in the unitarity limit [32, 73, 74], as we will further discuss in section 6. Note that many of the curves shown in figures 3 and 4 actually anticross when examined on a finer energy scale.

5. Three bosons

The wave function for three spinless bosons, $\psi_{\rm rel}(x,y) \equiv \psi_{3B}(x,y)$, must be symmetric under any particle permutation. The proper ansatz wave function is

$$\psi_{3B}(x,y) = (1 + \boldsymbol{P}_{13} + \boldsymbol{P}_{23})\,\Omega(x,y), \tag{40}$$

as $\Omega(x,y)$ is invariant under the permutation $1 \leftrightarrow 2$. The exchange operator $\boldsymbol{P}_{13}$ is the same as in the ansatz (28) for fermions, whereas $\boldsymbol{P}_{23}$ swaps atoms 2 and 3. The latter leads to the following coordinate transformation:

$$\begin{aligned} x &\to \frac{x}{2} - \frac{\sqrt{3}}{2} y \equiv \gamma, \\ y &\to -\frac{\sqrt{3}}{2} x - \frac{y}{2} \equiv \delta. \end{aligned} \tag{41}$$

Therefore, Eq. (40) may be explicitly written as

$$\psi_{3B}(x,y) = \Omega(x,y) + \Omega(\xi,\eta) + \Omega(\gamma,\delta). \tag{42}$$

As for fermions, it suffices to impose the contact condition (30) for particles 1 and 2,

$$\left[\frac{\partial \psi_{3B}(x,y)}{\partial x}\right]_{x\to 0^+} - \left[\frac{\partial \psi_{3B}(x,y)}{\partial x}\right]_{x\to 0^-} = 2g\,\psi_{3B}(0,y), \tag{43}$$

since the conditions for the other pairs are automatically satisfied through the exchange symmetry of (40). The required derivative is:

$$\frac{\partial \psi_{3B}(x,y)}{\partial x} = \frac{\partial \Omega(x,y)}{\partial x} + \frac{1}{2}\left[\frac{\partial \Omega(\xi,\eta)}{\partial \xi} + \sqrt{3}\frac{\partial \Omega(\xi,\eta)}{\partial \eta}\right] + \frac{1}{2}\left[\frac{\partial \Omega(\gamma,\delta)}{\partial \gamma} - \sqrt{3}\frac{\partial \Omega(\gamma,\delta)}{\partial \delta}\right]. \tag{44}$$

Since the only term that has a singular derivative in $x = 0$ is $\Omega(x, y)$, one proceeds as in the fermionic case obtaining

$$2g\sum_n a_n\left[\sqrt{\pi}\frac{\Gamma(-\nu_n)}{\Gamma(-\nu_n+1/2)}R_n(y) + 2\ \psi_n\left(\frac{\sqrt{3}}{2}y\right)R_n\Big(-\frac{y}{2}\Big)\right] = -4\sqrt{\pi}\sum_n a_n R_n(y). \tag{45}$$

Exploiting as before the orthonormality of the orbitals $R_n(y)$, the eigenvalue problem (45) is written as a set of linear equations,

$$\sum_n B_{mn}\, a_n = -\frac{2\sqrt{\pi}}{g}a_m, \tag{46}$$

with the matrix B_{mn} being defined as

$$B_{mn} = \sqrt{\pi}\frac{\Gamma(-\nu_n)}{\Gamma(-\nu_n+1/2)}\delta_{nm} + 2A_{mn}, \tag{47}$$

where A_{mn} is given in (39) and again the indices m and n assume either even or odd values depending on the parity of the bosonic state. The method to solve the eigenvalue problem (46) parallels that of section 4.

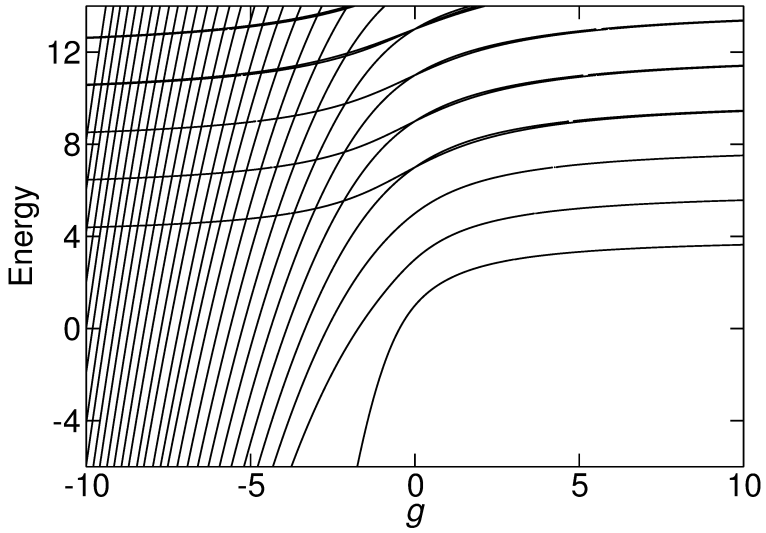

Figure 5. Energy of three bosons vs interaction strength g in the relative frame for states having even parity. The energy is in units of $\hbar\omega$ and g in units of $\hbar\omega\ell$.

Figures 5 and 6 show the energy spectra of three bosons obtained with $n_{\max} = 60$, whose wave functions have respectively even and odd parities. The plots are

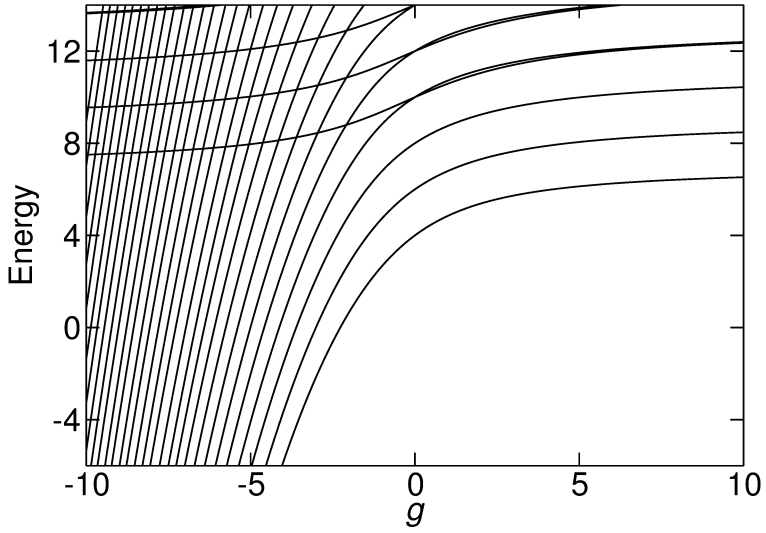

Figure 6. Energy of three bosons vs interaction strength g in the relative frame for states having odd parity. The energy is in units of $\hbar\omega$ and g in units of $\hbar\omega\ell$.

qualitatively similar to those for fermions (figures 3 and 4), displaying both dimer-atom energies that drop to $-\infty$ for increasing attractive interaction as well as energy branches that tend to fermionized values at unitarity (see also section 6). Contrary to the fermionic case, the ground state has now even parity, as it is clear for noninteracting particles all filling the lowest harmonic-oscillator state.

6. Strong repulsion

In the limit of strong repulsion, $g \to \infty$, bosons are predicted to fermionize, exhibiting the same observable properties as those of the dual system of fully spin-polarized fermions [17]. This is evident from figure 7, which displays the energy levels of three bosons as g increases up to 10^3. In this limit, all branches (continuous curves) tend to the noninteracting values of the system of three fermions having parallel spins (horizontal dashed lines), $E = 4, 6, 7, 8, \ldots$, confirming the accuracy of our calculation. Note that the missing value $E = 5$ is obtained when exciting a quantum of the center-of-mass motion.

The behavior of strongly repulsive fermions that are not spin-polarized is more involved, due to the emergence of a large degeneracy of levels at unitarity [28–32, 34, 73, 74]. This may be seen in figure 8, which shows that as $g \to \infty$ all energy levels tend to integer values that are twice or more degenerate asymptotically. Each one of these manifolds at $g = \infty$ includes at least one even (red [gray] curves) and one odd (black curves) state.

To rationalize this trend, consider the wave function of three fermions in the standard frame, $\Psi(x_1, \sigma_1; x_2, \sigma_2; x_3, \sigma_3)$, where x_i is the coordinate of the ith atom and $\sigma_i = \pm 1$ its spin projection. The contact condition enforcing Pauli exclusion principle is that $\Psi \equiv 0$ when $x_i = x_j$ and $\sigma_i = \sigma_j$, for any i, j. In addition, at unitarity one has $\Psi \equiv 0$ also when $x_i = x_j$ and $\sigma_i = -\sigma_j$ [73]. These two conditions, together with the mirror symmetry of the problem, imply that at unitarity both even

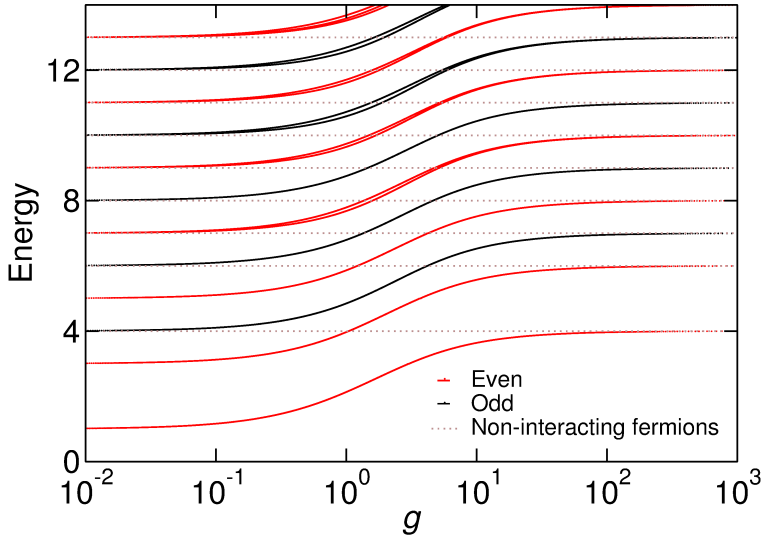

Figure 7. Energies of three bosons vs g for large repulsive interaction in the relative frame. Both even (red [gray] curves) and odd (black curves) states are considerd. Note the logarithmic scale of the g axis. The dotted horizontal lines point to the energies of three fully spin-polarized fermions. The energy is in units of $\hbar\omega$ and g in units of $\hbar\omega\ell$.

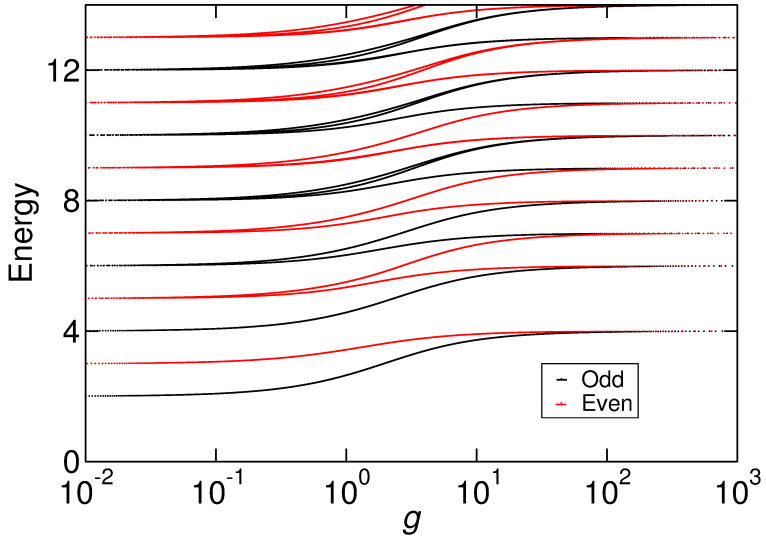

Figure 8. Energies of three fermions vs g for large repulsive interaction in the relative frame. Both even (red [gray] curves) and odd (black curves) states are considerd. Note the logarithmic scale of the g axis. The energy is in units of $\hbar\omega$ and g in units of $\hbar\omega\ell$.

Table 1. Size of CI subspace for three fermions vs single-particle basis set. The data refer to the odd-parity sector of total spin projection $S_z = \hbar/2$.

Number of orbitals	CI subspace size
10	450
25	7500
30	13 050
35	20 825
40	31 200
50	61 250

and odd states exhibit like nodal surfaces, owning the same probability density and energy.

7. Comparison with full configuration interaction

We have tested the results of our variational method (VM) with the data available in the literature. In particular, the energies of three fermions with odd parity agree with the values tabulated in Ref. [32] (Supplemental Material) to the sixth digit, the dataset including the ground state branch for $0 < g < \infty$ and the super-Tonks-Girardeau branch from $E = 4$ to $E = 6$ for $-\infty < g < 0$. On the other hand, our VM data for the three-fermion ground state energy significantly depart from those of Ref. [67]. After using the GNU sofware Plot Digitizer and considering the different unit length definition, we extract from figure 5 of Ref. [67] the values $E = 0.44$, 0.87, 1.25, 1.61, 2, 2.24, 2.48, 2.67, 2.84 for increasing values of g going from $g = -2.82843$ to $g = 2.82843$ in steps of $1/\sqrt{2}$, while the VM energies are $E = -3.08$, -1.21, 0.21, 1.26, 2, 2.49, 2.82, 3.05, 3.21 (cf. figure 3). The difference is huge especially at large negative values of g.

Using our VM data as a benchmark, in the following we discuss the convergence of the full CI method (also known as exact diagonalization), which is widely used for accurate calculations of energies and wave functions of few-body systems. The standard CI subspace for three fermions is spanned by the Slater determinants obtained by filling with three atoms—in all possible ways and consistently with Pauli exclusion principle—a truncated set of single-particle harmonic-oscillator orbitals. Table 1 reports the size of this CI subspace as the number of harmonic-oscillator orbitals increases. The full CI method provides a numerically exact solution in the limit of a complete single-particle basis set, the tradeoff for using a truncated basis set being the exponential growth of the CI subspace, as shown in table 1.

Figure 9 compares the VM energy spectrum for three fermions (solid curves) with selected CI data obtained from the home-made parallel code *DonRodrigo* [47] using 35 harmonic-oscillator orbitals (points). Since *DonRodrigo* uses the standard reference frame its output contains both relative-motion and center-of-mass excitations. To facilitate the comparison between CI and VM data, we have added the first two center-of-mass excitation quanta to the VM ground-state energy and included both parities in figure 9. CI predictions nicely match VM results for repulsive interactions, the smaller g the better the agreement. This converging behavior is generic to long-range repulsive interactions in one [36, 52, 53, 59, 60, 62, 64, 65] and two dimensions [46, 47, 81–84]. However, the performance of the CI method is poor on the attractive side, with

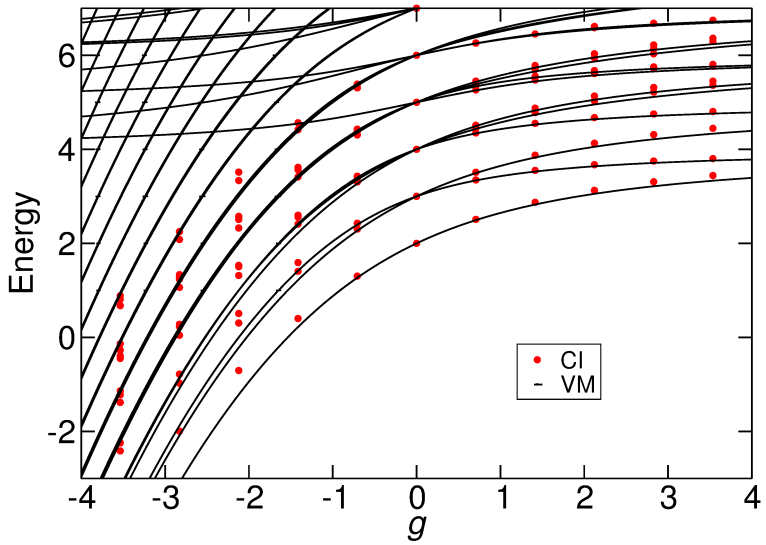

Figure 9. Energy spectrum of three fermions vs interaction strength g in the relative frame including both even and odd states. The total spin projection is $S_z = \hbar/2$. The data obtained from the variational method presented in this paper (VM, solid curves) are compared with those of a full-configuration-interaction calculation (CI, points). The latter method, also known as exact diagonalization, employed 35 harmonic-oscillator orbitals. The first two excitations of the center-of-mass motion from the absolute ground state were included in the plot to facilitate the comparison between the two techniques.

Table 2. Ground-state energies of three fermions in the relative frame for different interaction strengths g. The reference data obtained from the variational method (VM) presented in this work are compared with the results of full CI calculations using single-particle basis sets spanned by $n_{\rm SP}$ harmonic-oscillator orbitals. The size of the single-particle basis set, labeled as 'CI $n_{\rm SP}$', is indicated in the first row.

g	VM	CI 50	CI 40	CI 35	CI 30	CI 25
-2.8284	-3.0865	-2.1476	-2.0535	-1.9937	-1.9216	-1.8320
-2.1213	-1.2165	-0.7806	-0.7340	-0.7040	-0.6675	-0.6217
-1.4142	0.2185	0.3723	0.3897	0.4010	0.4149	0.4327
-1.0606	0.7890	0.8637	0.8725	0.8782	0.8853	0.8944
-0.7071	1.2685	1.2976	1.3011	1.3033	1.3062	1.3098
-0.3535	1.6695	1.6754	1.6762	1.6767	1.6773	1.6781
0.3535	2.2715	2.2755	2.2760	2.2764	2.2769	2.2775
0.7071	2.4935	2.5074	2.5093	2.5105	2.5120	2.5141
1.0606	2.6755	2.7016	2.7051	2.7074	2.7103	2.7142
1.4142	2.8255	2.8639	2.8691	2.8725	2.8769	2.8828
2.1213	3.0530	3.1138	3.1220	3.1275	3.1345	3.1439
2.8284	3.2140	3.2919	3.3024	3.3095	3.3186	3.3306

significant deviations from the VM predictions say for $g < -1.5$.

The slow convergence of the CI calculation for attractive interactions is detailed in table 2. The CI single-particle basis set is spanned by $n_{\rm SP}$ harmonic-oscillator orbitals. Increasing $n_{\rm SP}$ lowers systematically the ground-state energy as one moves

from the rightmost column of table 2 towards left for a certain value of g. However, whereas doubling $n_{\rm SP}$, going from 25 to 50, allows one to match the VM reference value at least with two-digit precision for all values of $g > 0$, this accuracy is obtained only for $g > -0.3535$ on the attractive side.

The reason is that attractive interactions squeeze the wave function probability weight at lower values of the relative distance x between two atoms. Therefore, the accuracy of the calculation crucially depends on the capability of the CI wave function to mimic the cusp of the exact wave function at $x = 0$, which occurs as an effect of the Bethe-Peierls contact condition. Since at the origin the exact wave function is not analytic, the CI single-particle basis set, spanned by smooth Hermite polynomials, badly performes and requires a large cutoff $n_{\rm SP}$ to reach reasonable accuracy. On the contrary, in the VM the wave function is expanded on a basis that includes the cusp from the beginning.

Among the strategies to improve the performance of the CI calculation, one possible route is to choose a different single-particle basis set. For example, using the eigenstates of the harmonic oscillator in the relative-motion frame we found a significant enhancement of convergence for two fermions. However, this path may be unpractical for more fermions, due to the complexity of two-body interaction matrix elements represented in this basis. Some authors proposed effective-interaction schemes or similar techniques borrowed by nuclear physics [85–88]. The interested reader may consult the recent review [89].

8. Conclusion

In this work we have obtained accurate energies for three particles interacting through contact forces in a one-dimensional harmonic trap. These results reproduce the exact beahvior in the limit of infinite interaction and may be used as a benchmark for other approximate theoretical treatments that are useful for larger systems. In particular, we find that the method of exact diagonalization, also known as full configuration interaction, converges slowly for strong attractive interactions between fermions. This points to the challenge of a numerical theory of pairing in finite one-dimensional systems that are currently under experimental investigation.

Acknowledgments

We thank Gerhard Zürn, Steffi Reimann, and Sven Åberg for stimulating discussions. This work is supported by the EU-FP7 Marie Curie initial training network INDEX and by the CINECA-ISCRA grants IscrC_TUN1DFEW and IscrC_TRAP-DIP.

Appendix A. Alternative solution of the two-body problem

In this appendix we solve the eigenvalue problem (6) in a manner alternative to that of section 2. Following the strategy concisely explained in [44], we write the relative-motion wave function as a linear combination of the harmonic-oscillator solutions $R_n(x)$ [cf. (7)]:

$$\psi(x) = \sum_{n=0}^{\infty} c_n R_n(x). \tag{A.1}$$

Inserting the representation (A.1) into the Hamiltonian (6) we obtain

$$\sum_{n=0}^{\infty} c_n(\epsilon_n - E_x)R_n(x) = -g\delta(x)\sum_{n=0}^{\infty} c_n R_n(x), \tag{A.2}$$

with $\epsilon_n = n + 1/2$, and projecting on the eigenstate $R_n(x)$ we get

$$c_n(\epsilon_n - E_x) + gR_n(0)\left[\sum_{m=0}^{\infty} c_m R_m(x)\right]_{x\to 0} = 0, \tag{A.3}$$

that can be written as

$$c_n = A\frac{R_n(0)}{\epsilon_n - E_x}, \tag{A.4}$$

with A being an unknown constant. We need only the even harmonic-oscillator solutions because the odd ones have value zero at $x = 0$ and correspond to noninteracting particles. Combining (A.3) and (A.4) we obtain the identity

$$-\frac{1}{g} = \left[\sum_{n=0}^{\infty}\frac{R_n(0)R_n(x)}{E_n - E_x}\right]_{x\to 0}. \tag{A.5}$$

The harmonic-oscillator orbitals may be written in terms of the Laguerre polynomials:

$$R_{2n}(x) = \frac{1}{\sqrt{\pi}}\frac{1}{R_{2n}(0)}\mathrm{e}^{-\frac{x^2}{2}}L_n^{-\frac{1}{2}}\big(x^2\big)\,. \tag{A.6}$$

Using this relation (A.5) takes the form

$$\begin{aligned}
-\frac{1}{g} &= \left[\frac{1}{\sqrt{\pi}}\mathrm{e}^{-\frac{x^2}{2}}\sum_{n=0}^{\infty}\frac{L_n^{-\frac{1}{2}}\big(x^2\big)}{\epsilon_{2n} - E_x}\right]_{x\to 0} = \\
&= \frac{1}{\sqrt{\pi}}\left[\mathrm{e}^{-\frac{x^2}{2}}\sum_{n=0}^{\infty}\frac{L_n^{-\frac{1}{2}}\big(x^2\big)}{2n + 1/2 - E_x}\right]_{x\to 0} = \\
&= \frac{1}{2\sqrt{\pi}}\left[\mathrm{e}^{-\frac{x^2}{2}}\sum_{n=0}^{\infty}\frac{L_n^{-\frac{1}{2}}\big(x^2\big)}{n - \nu}\right]_{x\to 0},
\end{aligned} \tag{A.7}$$

where $\nu = E_x/2 - 1/4$ and the dummy index runs over all n (even and odd) in the sum. To calculate the sum $\sum_n L_n^{-1/2}(x^2)/(n-\nu)$ we use the two following identities (cf. entry 22.9.15 in [78]):

$$\frac{1}{n-\nu} = \int_0^{\infty}\frac{\mathrm{d}y}{(1+y)^2}\left(\frac{y}{1+y}\right)^{n-\nu-1}, \tag{A.8}$$

$$\sum_{n=0}^{\infty} z^n L_n^{\alpha}(x) = (1-z)^{-\alpha-1}\exp\left(\frac{xz}{z-1}\right); \tag{A.9}$$

plus the tabulated integral (cf. entry 13.2.5 in [78]):

$$\int_0^{\infty}\frac{\mathrm{d}t}{(1+t)^{a+1-b}}\,t^{a-1}\mathrm{e}^{-zt} = \Gamma(a)\,U(a,b,z). \tag{A.10}$$

The final result is:

$$\sum_{n=0}^{\infty} \frac{L_n^{-\frac{1}{2}}(x^2)}{n-\nu} = \Gamma(-\nu)\, U\Big(-\nu, \frac{1}{2}, x^2\Big)\,. \tag{A.11}$$

From (13a) the limit of Kummer function $U(-\nu, 1/2, x^2)$ for $x \to 0$ is

$$\lim_{x\to 0} U\Big(-\nu, \frac{1}{2}, x^2\Big) = \frac{\Gamma(1/2)}{\Gamma\left(-\nu+1/2\right)}, \tag{A.12}$$

hence (A.7) becomes

$$-\frac{1}{g} = \frac{1}{2\sqrt{\pi}}\Gamma(-\nu)\frac{\Gamma(1/2)}{\Gamma\left(-\nu+1/2\right)}. \tag{A.13}$$

Therefore, we recover the eigenvalue equation (16), and plugging the identities (A.4), (A.6) and (A.11) into the expansion (A.1) we obtain the explicit form of the wave function:

$$\psi(x) = \frac{A}{2\sqrt{\pi}}\, \mathrm{e}^{-\frac{x^2}{2}}\, \Gamma(-\nu)\, U\Big(-\nu, \frac{1}{2}, x^2\Big)\,, \tag{A.14}$$

where the constant A is fixed by the normalization condition.

Appendix B. Explicit form of matrix element A_{pq}

We rewrite the matrix element (39) to evaluate:

$$A_{pq} = \int_{-\infty}^{+\infty} \mathrm{d}y R_p(y)\, \psi_q\Big(\frac{\sqrt{3}}{2}y\Big)\, R_q\Big(-\frac{y}{2}\Big)\,. \tag{B.1}$$

Writing the harmonic oscillator orbital as

$$R_n(z) = C_n \mathrm{e}^{-\frac{z^2}{2}} H_n(z)\,, \tag{B.2}$$

with

$$C_n = \frac{1}{\sqrt{2^n n!}}\left(\frac{1}{\pi}\right)^{\frac{1}{4}}, \tag{B.3}$$

the integral reads:

$$\begin{aligned} A_{pq} &= \int_{-\infty}^{+\infty} \mathrm{d}y\, C_p \mathrm{e}^{-\frac{y^2}{2}} \mathrm{e}^{-\frac{3}{8}y^2} \Gamma(-\nu_q) C_q \mathrm{e}^{-\frac{y^2}{8}} J_{pq}(y) \\ &= 2C_p\, C_q\, \Gamma(-\nu_q) \int_0^{\infty} \mathrm{d}y\, \mathrm{e}^{-y^2} J_{pq}(y), \end{aligned} \tag{B.4}$$

where

$$J_{pq}(y) = H_p(y)\, U\left(-\nu_q, 1/2, 3y^2/4\right) H_q(-y/2)\,. \tag{B.5}$$

Using the identity

$$\Gamma(a) U\left(a, \frac{1}{2}, z\right) = \sum_{k=0}^{\infty} \frac{L_k^{-\frac{1}{2}}(z)}{k+a} = \sum_{k=0}^{\infty} \frac{(-1)^k U(-k, 1/2, z)}{k!(k+a)}, \tag{B.6}$$

we rewrite the matrix element in the following way:

$$A_{pq} = 2C_p C_q \sum_{k=0}^{\infty} \frac{(-1)^k}{k!(k-\nu_q)} \int_0^{\infty} \mathrm{d}y\, I_{pq}^k(y), \tag{B.7}$$

where we have defined the integrand as

$$I^k_{pq}(y) = \mathrm{e}^{-y^2} H_p(y)\, U\left(-k, \frac{1}{2}, \frac{3}{4}y^2\right) H_q\left(-\frac{y}{2}\right). \tag{B.8}$$

The expression (B.7) has the advantage that it depends on the energy only through the parameter ν_q that enters the denominator of the addendum of the sum over k. Therefore, one computes and stores the integrals $\int \mathrm{d}y I^k_{pq}(y)$ once for all while repeating the summation over k for different energies, which makes the computation fast. In this way we performed calculations truncating the sum (B.7) up to $k = 30$ and obtaining convergence on the sixth digit of the ground state energy.

References

[1] P. Cheinet, S. Trotzky, M. Feld, U. Schnorrberger, M. Moreno-Cardoner, S. Fölling, and I. Bloch. *Phys. Rev. Lett.*, 101:090404, 2008.
[2] S. Will, T. Best, U. Schneider, L. Hackermüller, D.-S. Lühmann, and I. Bloch. *Nature (London)*, 465:197, 2010.
[3] F. Serwane, G. Zürn, T. Lompe, T. B. Ottenstein, A. N. Wenz, and S. Jochim. *Science*, 332:336, 2011.
[4] G. Zürn, F. Serwane, T. Lompe, A. N. Wenz, M. G. Ries, J. E. Bohn, and S. Jochim. *Phys. Rev. Lett.*, 108:075303, 2012.
[5] G. Zürn, A. N. Wenz, S. Murmann, T. Lompe, and S. Jochim. *Phys. Rev. Lett.*, 111:175302, 2013.
[6] A. N. Wenz, G. Zürn, , S. Murmann, I. Brouzos, T. Lompe, and S. Jochim. *Science*, 342:457, 2013.
[7] C. Chin, R. Grimm, P. Julienne, and E. Tiesinga. *Rev. Mod. Phys.*, 82:1225, 2010.
[8] T. Giamarchi. *Quantum physics in one dimension*. Clarendon, Oxford, 2003.
[9] S. Giorgini, L. P. Pitaevskii, and S. Stringari. *Rev. Mod. Phys.*, 80:1215, 2008.
[10] I. Bloch, J. Dalibard, and W. Zwerger. *Rev. Mod. Phys.*, 80:885, 2008.
[11] V. V. Deshpande, M. Bockrath, L. I. Glazman, and A. Yacobi. *Nature (London)*, 464:209, 2010.
[12] S. Ilani and P. L. McEuen. *Annu. Rev. Condens. Matter Phys.*, 1:1, 2010.
[13] M. A. Cazalilla, R. Citro, T. Giamarchi, E. Orignac, and N. Rigol. *Rev. Mod. Phys.*, 83:1405, 2011.
[14] X.-W. Guan, M. T. Batchelor, and C. Lee. *Rev. Mod. Phys.*, 85:1633, 2013.
[15] T. Kinoshita, T. Wenger, and D. S. Weiss. *Science*, 305:1125, 2004.
[16] B. Paredes, A. Widera, V. Murg, O. Mandel, S. Fölling, I. Cirac, G. V. Shlyapnikov, T. W. Hänsch, and I Bloch. *Nature (London)*, 429:277, 2004.
[17] M. Girardeau. *J. Math. Phys. (N.Y.)*, 1:516, 1960.
[18] T. Cheon and T. Shigehara. *Phys. Rev. Lett.*, 82:2536, 1999.
[19] A. Schirotzek, C.-H. Wu, A. Sommer, and M. W. Zwierlein. *Phys. Rev. Lett.*, 102:230402, 2009.
[20] M. Koschorreck, D. Pertot, E. Vogt, B. Fröhlich, M. Feld, and M. Köhl. *Nature (London)*, 485:619, 2012.
[21] C. Kohstall, M. Zaccanti, M. Jag, A. Trenkwalder, P. Massignan, G. M. Bruun, F. Schreck, and R. Grimm. *Nature (London)*, 485:615, 2012.
[22] J. Bardeen, L. N. Cooper, and J. R. Schrieffer. *Phys. Rev.*, 108:1175, 1957.
[23] A. J. Leggett. *Quantum liquids*. Oxford University Press, Oxford, 1st edition, 2006.
[24] C. A. Regal, C. Ticknor, J. L. Bohn, and D. S. Jin. *Nature (London)*, 424:47, 2003.
[25] M. Bartenstein, A. Altmeyer, S. Riedl, S. Jochim, C. Chin, J. Hecker Denschlag, and R. Grimm. *Phys. Rev. Lett.*, 92:120401, 2004.
[26] M. W. Zwierlein, J. R. Abo-Shaeer, A. Schirotzek, C. H. Schunck, and W. Ketterle. *Nature (London)*, 435:1047, 2005.
[27] X. Liu, H. Hu, and P. D. Drummond. *Phys. Rev. A*, 82:023619, 2010.
[28] P. O. Bugnion and G. J. Conduit. *Phys. Rev. A*, 87:060502(R), 2013.
[29] E. J. Lindgren, J. Rotureau, C. Forssén, A. G. Volosniev, and N. T. Zinner. arXiv:1304.2992, 2013.
[30] X. Cui and T.-L. Ho. arXiv:1305.6361, 2013.
[31] T. Sowiński, T. Grass, O. Dutta, and M. Lewenstein. *Phys. Rev. A*, 88:033607, 2013.
[32] S. E. Gharashi and D. Blume. *Phys. Rev. Lett.*, 111:045302, 2013.
[33] P. O. Bugnion and G. J. Conduit. *Phys. Rev. A*, 88:013601, 2013.

[34] A. G. Volosniev, D. V. Federov, A. S. Jensen, M. Valiente, and N. T. Zinner. arXiv:1306.4610, 2013.
[35] J. C. Cremon, G. M. Bruun, and S. M. Reimann. *Phys. Rev. Lett.*, 105:255301, 2010.
[36] J.-J. Wang, W. Li, S. Chen, Gao Xianlong, M. Rontani, and M. Polini. *Phys. Rev. B*, 86:075110, 2012.
[37] M. Rontani. *Phys. Rev. Lett.*, 108:115302, 2012.
[38] M. Rontani. *Phys. Rev. A*, 88:043633, 2013.
[39] P. O. Bugnion, J. A. Lofthouse, and G. J. Conduit. *Phys. Rev. Lett.*, 111:045301, 2013.
[40] M. Rontani, J. R. Armstrong, Y. Yu, S. Åberg, and S. M. Reimann. *Phys. Rev. Lett.*, 102:060401, 2009.
[41] M. A. Garcia-March, B. Julia-Diaz, G. E. Astrakharchik, T. Busch, J. Boronat, and A. Polls. *Phys. Rev. A*, 88:063604, 2013.
[42] D. Blume. *Rep. Prog. Phys.*, 75:046401, 2012.
[43] N. T. Zinner and A. S. Jensen. *J. Phys. G: Nucl. Part. Phys.*, 40:053101, 2013.
[44] T. Busch, B.-G. Englert, K. Rzążewski, and M. Wilkens. *Found. Phys.*, 28:549, 1998.
[45] X. Liu, H. Hu, and P. D. Drummond. *Phys. Rev. B*, 82:054524, 2010.
[46] S. M. Reimann and M. Manninen. *Rev. Mod. Phys.*, 74:1283, 2002.
[47] M. Rontani, C. Cavazzoni, D. Bellucci, and G. Goldoni. *J. Chem. Phys.*, 124:124102, 2006.
[48] D. M. Ceperley. *Rev. Mod. Phys.*, 67:279, 1995.
[49] G. E. Astrakharchik, D. Blume, S. Giorgini, and B. E. Granger. *Phys. Rev. Lett.*, 92:030402, 2004.
[50] M. Casula, D. M. Ceperley, and E. J. Mueller. *Phys. Rev. A*, 78:033607, 2008.
[51] G. E. Astrakharchik and I. Brouzos. arXiv:1303.7007, 2013.
[52] G. W. Bryant. *Phys. Rev. Lett.*, 59:1140, 1987.
[53] W. Häusler and B. Kramer. *Phys. Rev. B*, 47:16353, 1993.
[54] B. Szafran, F. M. Peeters, S. Bednarek, T. Chwiej, and J. Adamowski. *Phys. Rev. B*, 70:035401, 2004.
[55] G. A. Fiete, J. Qian, Y. Tserkovnyak, and B. I. Halperin. *Phys. Rev. B*, 72:045315, 2005.
[56] Y. Gindikin and V. A. Sablikov. *Phys. Rev. B*, 76:045122, 2007.
[57] F. Deuretzbacher, K. Bongs, K. Sengstock, and D. Pfannkuche. *Phys. Rev. A*, 75:013614, 2007.
[58] X. Yin, Y. Hao, S. Chen, and Y. Zhang. *Phys. Rev. A*, 78:013604, 2008.
[59] A. Secchi and M. Rontani. *Phys. Rev. B*, 80:041404(R), 2009.
[60] A. Secchi and M. Rontani. *Phys. Rev. B*, 82:035417, 2010.
[61] L. H. Kristinsdóttir, J. C. Cremon, H. A. Nilsson, H. Q. Xu, L. Samuelson, H. Linke, A. Wacker, and S. M. Reimann. *Phys. Rev. B*, 83:041101(R), 2011.
[62] A. Secchi and M. Rontani. *Phys. Rev. B*, 85:121410(R), 2012.
[63] I. Brouzos and P. Schmelcher. *Phys. Rev. Lett.*, 108:045301, 2012.
[64] S. Pecker, F. Kuemmeth, A. Secchi, M. Rontani, D. C. Ralph, P. L. McEuen, and S. Ilani. *Nature Phys.*, 9:576, 2013.
[65] A. Secchi and M. Rontani. *Phys. Rev. B*, 88:125403, 2013.
[66] S. E. Gharashi, K. M. Daily, and D. Blume. *Phys. Rev. A*, 86:042702, 2012.
[67] N. L. Harshman. *Phys. Rev. A*, 86:052122, 2012.
[68] B. Wilson, A. Foerster, C. C. N. Kuhn, I. Roditi, and D. Rubeni. arXiv:1307.1180, 2013.
[69] S. Zöllner, H.-D. Meyer, and P. Schmelcher. *Phys. Rev. A*, 74:053612, 2006.
[70] T. Ernst, D. W. Hallwood, J. Gulliksen, H.-D. Meyer, and J. Brand. *Phys. Rev. A*, 84:023623, 2011.
[71] I. Brouzos and P. Schmelcher. *Phys. Rev. A*, 87:023605, 2013.
[72] Gao Xianlong, M. Polini, R. Asgari, and M. P. Tosi. *Phys. Rev. A*, 73:033609, 2006.
[73] L. Guan, S. Chen, Y. Wang, and Z.-Q. Ma. *Phys. Rev. Lett.*, 102:160402, 2009.
[74] M. Girardeau. *Phys. Rev. A*, 82:011607(R), 2010.
[75] C. J. Pethick and H. Smith. *Bose-Einstein Condensation in Dilute Gases*. Cambridge University Press, Cambridge (UK), 2001.
[76] M. Olshanii. *Phys. Rev. Lett.*, 81:938, 1998.
[77] H. Bethe and R. Peierls. *Proc. R. Soc. Lond. A*, 148:146, 1935.
[78] M. Abramowitz and I. A. Stegun. *Handbook of Mathematical Functions*. Dover Edition, New York, 1964.
[79] G. E. Astrakharchik, J. Boronat, J. Casulleras, and S. Giorgini. *Phys. Rev. Lett.*, 95:190407, 2005.
[80] M. Girardeau and G. E. Astrakharchik. *Phys. Rev. A*, 81:061601(R), 2010.
[81] J. I. Climente, A. Bertoni, G. Goldoni, M. Rontani, and E. Molinari. *Phys. Rev. B*, 76:085305, 2007.

[82] S. Kalliakos, M. Rontani, V. Pellegrini, C. P. Garcia, A. Pinczuk, G. Goldoni, E. Molinari, L. N. Pfeiffer, and K. W. West. *Nature Phys.*, 4:467, 2008.
[83] A. Singha, V. Pellegrini, A. Pinczuk, L. N. Pfeiffer, K. W. West, and M. Rontani. *Phys. Rev. Lett.*, 104:246802, 2010.
[84] A. Gamucci, V. Pellegrini, A. Singha, A. Pinczuk, L. N. Pfeiffer, K. W. West, and M. Rontani. *Phys. Rev. B*, 85:033307, 2012.
[85] S. Kvaal, M. Hjorth-Jensen, and H. M. Nilsen. *Phys. Rev. B*, 76:085421, 2007.
[86] I. Stetcu, B. R. Barret, U. van Kolck, and J. P. Vary. *Phys. Rev. A*, 76:063613, 2007.
[87] Y. Alhassid, G. F. Bertsch, and L. Fang. *Phys. Rev. Lett.*, 100:230401, 2008.
[88] J. Christensson, C. Forssén, S. Åberg, and S. M. Reimann. *Phys. Rev. A*, 79:012707, 2009.
[89] J. Mitroy, S. Bubin, W. Horiuchi, Y. Suzuki, L. Adamowicz, W. Cencek, K. Szalewicz, J. Komasa, D. Blume, and K. Varga. *Rev. Mod. Phys.*, 85:693, 2013.